AD-A080 095 PURDUE UNIV LAFAYETTE IN TURNER LAB FOR ELECTROCERAMICS F/G 9/1
THE EFFECTS OF SUBSTRATE COMPOSITION ON THICK FILM CIRCUIT RELI--ETC(U)
NOV 79 R W VEST N00019-79-C-0240

UNCLASSIFIED NL

1 OF 1
AD A 080095

END
DATE FILMED
2 — 80
DDC

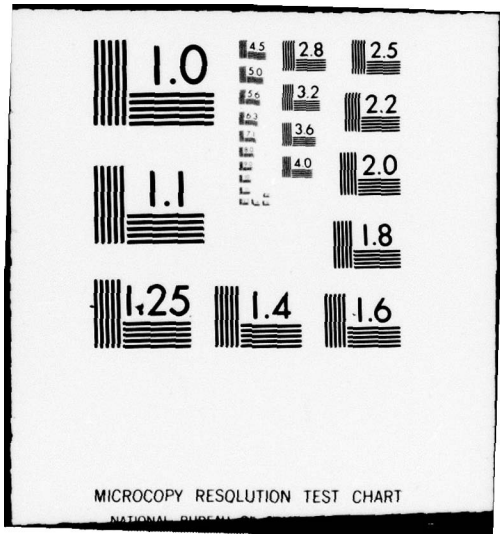
1.0
1.1
1.25
1.4
1.6
1.8
2.0
2.2
2.5
2.8
3.2
3.6
4.0
4.5
5.0
5.6
MICROCOPY RESOLUTION TEST CHART

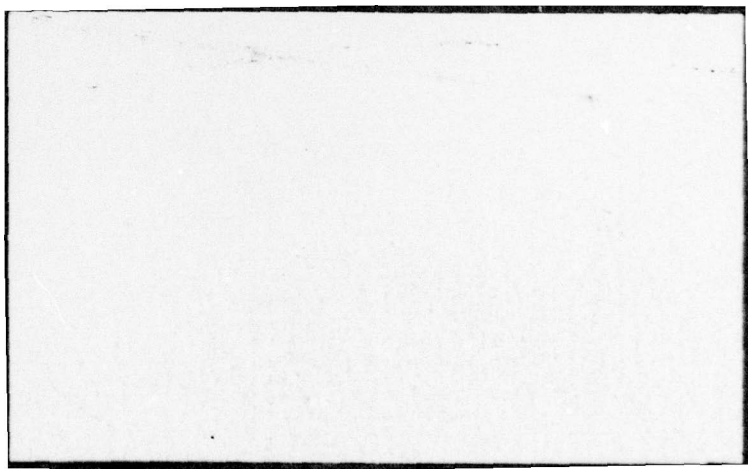

(12)

(6) THE EFFECTS OF SUBSTRATE COMPOSITION ON THICK FILM CIRCUIT RELIABILITY.

(10) R. W. Vest

(11) 30 Nov[illegible]79

(12) 31

Quarterly Report No. 3

For the period 8/1/79-10/31/79

Contract No. N0019-79-C-0240

Prepared for

NAVAL AIR SYSTEMS COMMAND (15) N0019-79-C-0240

(9) Quarterly rept. no. 3, 1 Aug-31 Oct 79,

410 421

FOREWORD

Research described in this report constitutes the third three months of effort under Contract No. N0019-79-C-0240 with the Naval Air Systems Command, Department of the Navy, under the technical cognizance of James Willis. The research was conducted in the Turner Laboratory for Electroceramics, School of Materials Engineering and School of Electrical Engineering, Purdue University, West Lafayette, Indiana 47907, under the direction of Professor R. W. Vest. Contributing to the project were Messrs. P. Palanisamy, R. L. Reed, and C-T. Tarn.

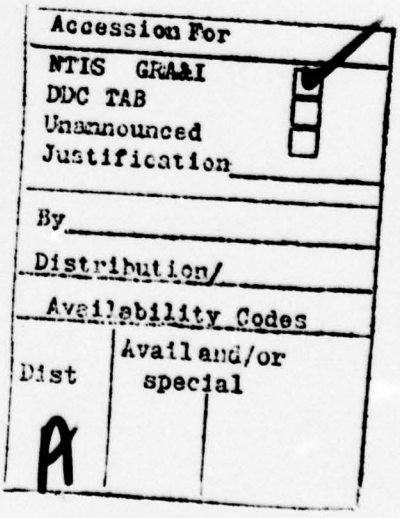

SECURITY CLASSIFICATION OF THIS PAGE (When Data Entered)

REPORT DOCUMENTATION PAGE		READ INSTRUCTIONS BEFORE COMPLETING FORM
1. REPORT NUMBER 3	2. GOVT ACCESSION NO.	3. RECIPIENT'S CATALOG NUMBER
4. TITLE (and Subtitle) THE EFFECTS OF SUBSTRATE COMPOSITION ON THICK FILM CIRCUIT RELIABILITY		5. TYPE OF REPORT & PERIOD COVERED Quarterly 8/1/79-10/31/79
		6. PERFORMING ORG. REPORT NUMBER
7. AUTHOR(s) R. W. Vest		8. CONTRACT OR GRANT NUMBER(s) N0019-79-C-0240
9. PERFORMING ORGANIZATION NAME AND ADDRESS PURDUE RESEARCH FOUNDATION, PURDUE UNIVERSITY, West Lafayette, Indiana 47907		10. PROGRAM ELEMENT, PROJECT, TASK AREA & WORK UNIT NUMBERS
11. CONTROLLING OFFICE NAME AND ADDRESS NAVAL AIR SYSTEMS COMMAND, AIR 310B Washington, D.C. 20361		12. REPORT DATE 30 November 1979
		13. NUMBER OF PAGES 25
14. MONITORING AGENCY NAME & ADDRESS(if different from Controlling Office)		15. SECURITY CLASS. (of this report) Unclassified
		15a. DECLASSIFICATION/DOWNGRADING SCHEDULE N/A

16. DISTRIBUTION STATEMENT (of this Report)

APPROVED FOR PUBLIC RELEASE;
DISTRIBUTION UNLIMITED

17. DISTRIBUTION STATEMENT (of the abstract entered in Block 20, if different from Report)

18. SUPPLEMENTARY NOTES

19. KEY WORDS (Continue on reverse side if necessary and identify by block number)

Thick Film Resistors	Electronic Glass
Ceramic Substrates	Sintering
Electrical Resistivity	Ripening

20. ABSTRACT (Continue on reverse side if necessary and identify by block number)

Measurements of the density of, and the ripening of RuO_2 in, thick film glasses as a function of temperature and amount of AlSiMag 614 (96% Al_2O_3) substrate dissolved in the glasses were conducted. The minor constituents (4%) in the substrate were found to have an anomalously large effect on the density. The ripening results were interpreted in terms of a phase boundary reaction rate limiting step, and the transfer coefficient was calculated from the data. A theoretical equation was derived for the

DD FORM 1 JAN 73 1473 EDITION OF 1 NOV 65 IS OBSOLETE
S/N 0102-014-6601

SECURITY CLASSIFICATION OF THIS PAGE (When Data Entered)

20. Abstract (Continued)

initial stage sintering kinetics of RuO_2 in the glass. This equation was combined with the results of the ripening study to predict the neck growth between RuO_2 particles as a function of temperature and amount of dissolved substrate.

TABLE OF CONTENTS

1. INTRODUCTION

The print and fire processing of thick film circuits ensures that there always will be some degree of chemical interaction between the film and the substrate, because all common substrate materials are soluble to some degree in the glasses used in thick film inks. This interaction is primarily responsible for the development of adhesion between the thick film and the substrate, but it also leads to changes in the composition of the glass with the net result that the physical properties of the glass will change. These changes in physical properties of the glass will result in modified kinetics for the various microstructure development processes and all electrical properties of the resistors are related to the microstructure. The goal of this research program is to develop a sufficient level of understanding of the phenomena involved so that appropriate models can be developed. These models should lead to the writing of specifications for impurity limits and additive ranges for substrates, and to recommendations concerning glass composition and processing conditions.

Previously reported studies [1-5] under this program have established the magnitude of the effects resulting from chemical interaction between a thick film resistor and a ceramic substrate, and have determined the specific influence on important properties of the resistor glass. The rates of dissolution of two substrates, 96% Al_2O_3 (AlSiMag 614) and 99.5% Al_2O_3 (AlSiMag 772), in two lead borosilicate glasses (63 w/o PbO-25 w/o B_2O_3-12 w/o SiO_2 and 70 w/o PbO-20 w/o B_2O_3-10 w/o SiO_2) were measured at various temperatures. The rate limiting steps for each substrate-glass system were determined in all appropriate temperature ranges, and analytical equations

were developed to predict the substrate recession as a function of time and temperature for thick film resistors. The saturation solubility of AlSiMag 614 substrates in 63-25-12 glass was determined as a function of temperature, and these results were combined with the dissolution rate studies in order to test various kinetic models. Studies of the kinetics of initial stage sintering of glass particles were conducted in order to determine the ratio of surface tension to viscosity for the two standard glasses, and the standard glasses with additions of substrate ingredients. Both the magnitude and the activation energies of this ratio were found to be significantly different for the glasses, confirming the extreme sensitivity of this parameter to small changes in glass composition. The viscosity of the 63-25-12 glass was measured as a function of amount of dissolved AlSiMag 614 substrate from 450° to 850°C. The isothermal viscosity was found to increase by a factor of 20 with 10 w/o dissolved substrate relative to the standard lead borosilicate glass. The surface tension of the 63-25-12 glass was measured as a function of the amount of dissolved AlSiMag 614 substrate from 600°C to 900°C. The surface tension increased with increasing amount of dissolved substrate with the effect being most pronounced at the higher temperatures. The effects of the minor constituents (4%) in the AlSiMag 614 substrate composition on viscosity and surface tension of the glasses was determined to be larger than predictions based on the principal of additivity. The sheet resistance, temperature dependence of resistance, and the current noise were measured for thick film resistors as a function of the amount of substrate dissolved in the resistor for various firing temperatures at constant firing time, and for various firing times at 800°C. Large variations in these three properties were observed, and the changes were

qualitatively correlated with changes in viscosity of the glass. The microstructure development and charge transport models used to correlate the results indicated a retardation of microstructure development in the resistors as the amount of dissolved substrate increased which led to changing proportions of sintered and non-sintered contacts in the RuO_2 networks within the body of the resistor. The non-sintered contacts were modeled using MIM devices, and the dominant charge transport mechanism for glass films >7 nm at room temperature and above was Schottky emission, while quantum mechanical tunneling became important for thinner films and/or lower temperatures.

2. DENSITY OF GLASSES

The dissolution of AlSiMag 614 (96% Al_2O_3) substrate in the standard glass (63 w/o PbO-25 w/o B_2O_3-12 w/o SiO_2) was shown [2] to proceed through molecular diffusion and free convection as rate limiting steps. Free convection could be caused by gradients in temperature, surface tension, or density due to the dissolution of substrate in the glass. Convection due to temperature differences caused by the reaction can be considered negligible because the experiments were carried out at sufficiently high temperatures ($\geq 760^{o}C$) that any thermal gradients caused by the dissolution would have been balanced by heat radiation from the bulk glass. Surface tension effects need not be considered for these experiments because the substrates were completely immersed in the glass, which leaves density gradients as the most probable driving force for convection.

The density was determined as a function of composition and temperature in the gold sphere viscometer [4] utilizing Archimede's principle:

$$\text{Glass density} = \frac{(\text{weight in air} - \text{weight in glass})}{\text{weight in air}} \times \text{density of gold} \qquad (1)$$

The density results for the standard glass and four other compositions doped with AlSiMag 614 substrate or alumina are given in Fig. 1. The density (ρ) for each glass can be adequately represented as a linear function of absolute temperature (T) in the range measured. The densities in gm/cc are:

$$\text{Standard glass:} \quad \rho = 5.2607 - 1.1068 \times 10^{-3} T \qquad (2)$$

$$\text{6 w/o sub. glass:} \quad \rho = 4.6997 - 7.6200 \times 10^{-4} T \qquad (3)$$

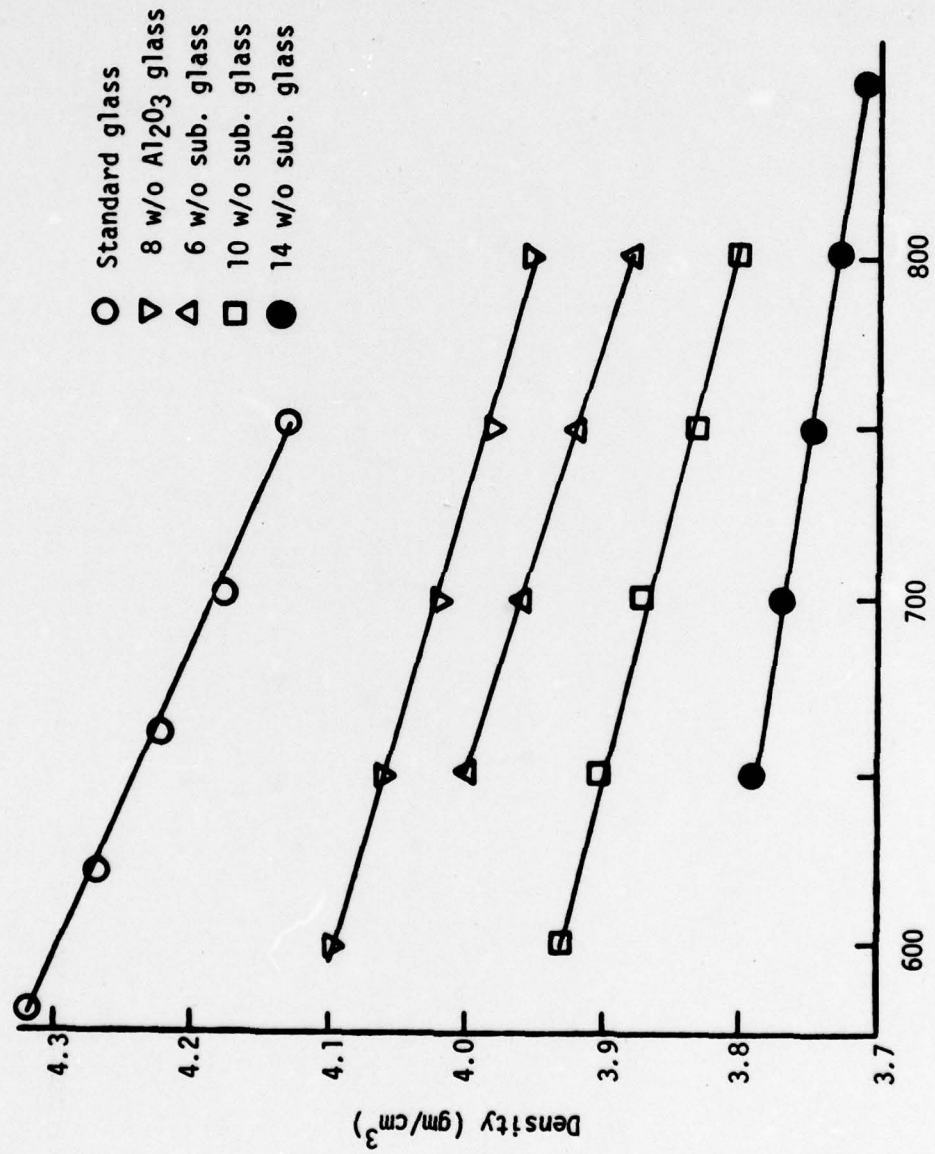

Figure 1. Variation of Glass Density with Composition and Temperature.

10 w/o sub. glass: $\rho = 4.5096 - 6.6000 \times 10^{-4} T$ (4)

14 w/o sub. glass: $\rho = 4.1457 - 3.8800 \times 10^{-4} T$ (5)

8 w/o Al_2O_3 glass: $\rho = 4.7163 - 7.1400 \times 10^{-4} T$ (6)

The decrease in density of the glass due to substrate dissolution is sufficiently large to lead to density gradients which could be responsible for the natural convection following the molecular diffusion process during the dissolution of the substrate. The temperature coefficient of density, for the temperature range investigated, is seen to decrease with increasing additions of substrate.

A comparison of the density of the 8 w/o Al_2O_3 glass with the substrate glasses in Fig. 1 shows that the minor constituents (3.6% SiO_2, 1.3% MgO, 0.1% CaO, 0.2% Fe_2O_3) in the AlSiMag 614 substrate have a significant effect. The density of a liquid may be approximated to be an additive property of its constituents, but nonlinear behavior would be expected if the constituents differ greatly in density or if there is a change in the structure of the liquid due to the addition. Additivity factors for room temperature density based on percent by weight of PbO, B_2O_3, SiO_2, and Al_2O_3 have been reported [6] to be 9.6, 1.9, 2.3, and 4.1, respectively. Addition of Al_2O_3 to a high lead glass would be expected to decrease the density, and addition of SiO_2 would bring the density down even further. Thus the additivity factors qualitatively explain the fact that the addition of substrate lowers the density more than the addition of an equal amount of pure Al_2O_3 However, the differences cannot be quantitatively accounted for by considering additivity factors alone; possible differences in glass structure, as indicated by the anomalous behavior of the viscosity of 8 w/o Al_2O_3 glass [3], may be responsible for the observed anomaly in density.

3. RuO_2 RIPENING

The experimental techniques and some preliminary results for studies of the rate of dissolution of small particles and growth of large particles (ripening) of RuO_2 in glass were previously presented [4]. The complete results of surface area measurements on RuO_2 samples held for varying times in the standard, 2 w/o, 4 w/o, and 10 w/o substrate doped glasses at 950°C are given in Fig. 2. The extensive measurements of RuO_2 particle growth in the standard and 10 w/o substrate glasses showed that after a rapid decrease, the surface area decreased very slowly at longer times. The results also indicate that the ripening process is considerably retarded by the addition of substrate to the standard glass. The amount of RuO_2 relative to the glasses was varied from 20 to 30 w/o for the standard and 10 w/o substrate doped glasses, and the effect of this variation on the ripening kinetics is seen to be insignificant. For ripening studies at 888° and 1000°C, composites made of RuO_2 and the standard, 4 w/o, 10 w/o, and 14 w/o substrate doped glasses were used in order to cover a wider glass composition range.

If diffusion controlled solution-precipitation is the rate limiting step for the process of ripening of solid particles dispersed in a continuous matrix, the average particle radius obeys the following time dependence.

$$[\bar{r}\ (t)]^3 - [\bar{r}\ (o)]^3 = \left[\frac{8}{9}\frac{C_o \gamma_{sl} V_o^2 D}{RT}\right] t \qquad (7)$$

In this equation, $\bar{r}$ (t) is the average particle radius at time t, $\bar{r}$ (o) is the average particle radius at time zero, C_o is the equilibrium solubility, γ_{sl} is the solid-liquid interfacial energy, V_o is the molar volume, D is

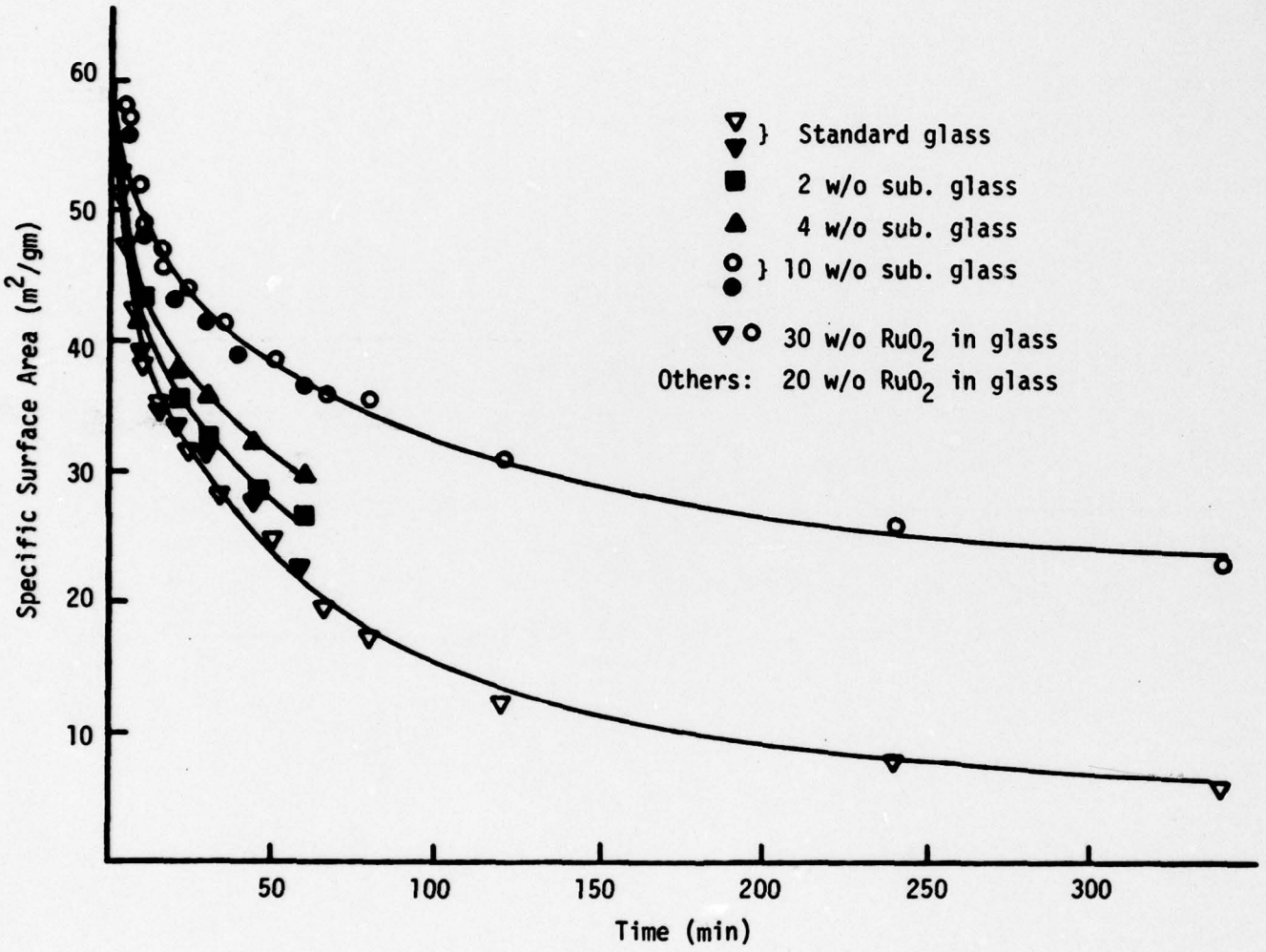

Figure 2. Ripening of RuO_2 in Glasses at 950°C.

the diffusion coefficient, and R is the gas constant. If the particle growth occurs by a phase boundary reaction controlled solution-precipitation process, the average particle radius increases according to

$$[\bar{r}\ (t)]^2 - [\bar{r}\ (o)]^2 = \left[\left(\frac{8}{9}\right)^2 \frac{C_o \gamma_{sl} V_o^{\ 2} K_T}{RT}\right] t \qquad (8)$$

where K_T is the transfer coefficient. Lease squares fits, of the experimental data, to these equations for varying glass compositions at three different temperatures indicated that the interface reaction is the slowest step of mass transport in this system. Plots of $([r\ (t)]^2 - [r\ (o)]^2)$ versus time are are straight lines for all the three temperatures investigated as shown in Figs. 3-5. The slopes of the lines, which are proportional to $C_o \gamma_{sl} K_T$, are significantly reduced by the addition of substrate to the standard glass. The values of $C_o \gamma_{sl} K_T$ were calculated from the slopes, and least squares analyses on the data to an Arrhenius fit were performed to give the following equations:

Standard glass: $C_o \gamma_{sl} K_T = 8.577 \times 10^6 \exp [-(51601 \pm 6416)/T]$ (9)

4 w/o sub. glass: $C_o \gamma_{sl} K_T = 6.533 \times 10^5 \exp [-(49187 \pm 7559)/T]$ (10)

10 w/o sub, glass: $C_o \gamma_{sl} K_T = 9.206 \times 10^4 \exp [-(47637 \pm 6796)/T]$ (11)

14 w/o sub. glass: $C_o \gamma_{sl} K_T = 5.305 \times 10^5 \exp [-50085/T]$ (12)

In these equations, C_o is in gm/cc, γ_{sl} in J/cm^2, and K_T in cm/s. An average exponential term of -49626/T was selected to represent all four compositions because the differences among the individual glasses were within

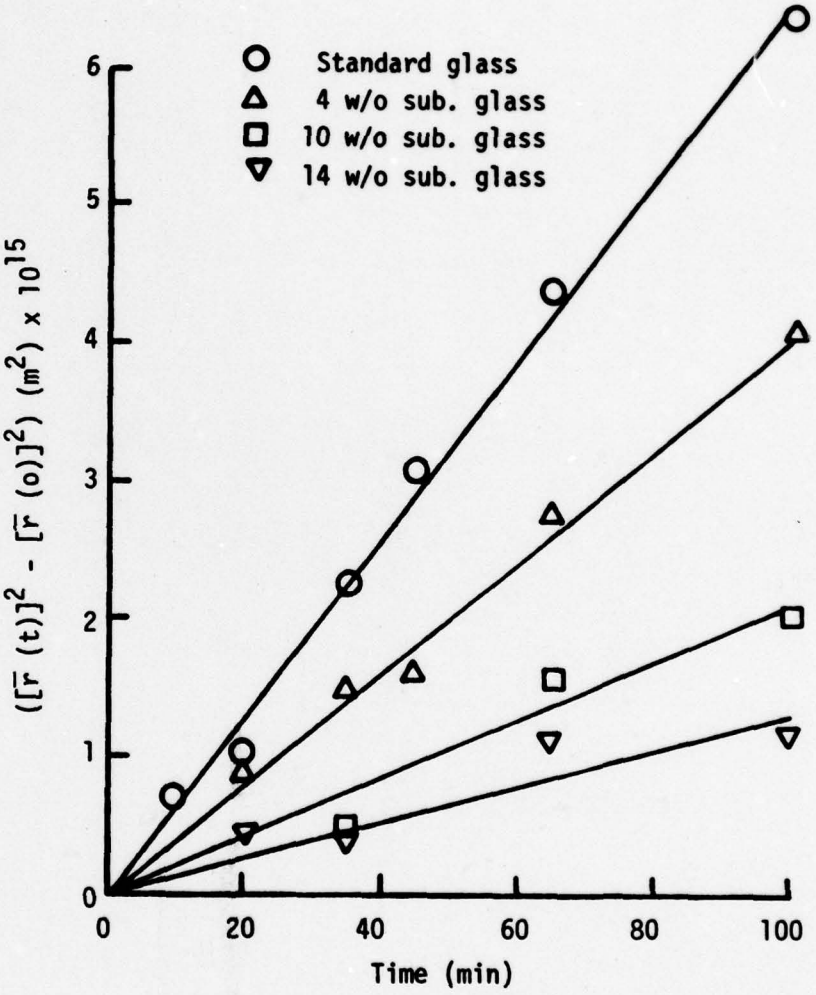

Figure 3. RuO_2 Ripening in Glasses at 888°C.

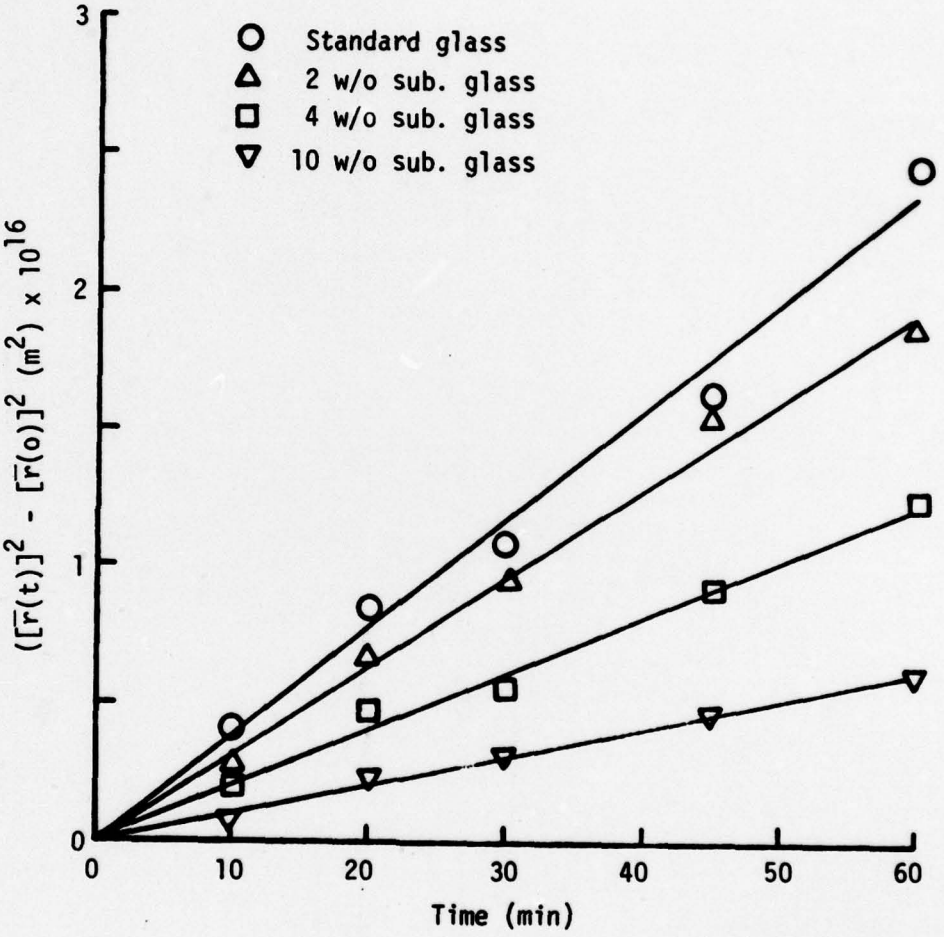

Figure 4. RuO_2 Ripening in Glasses at 950°C.

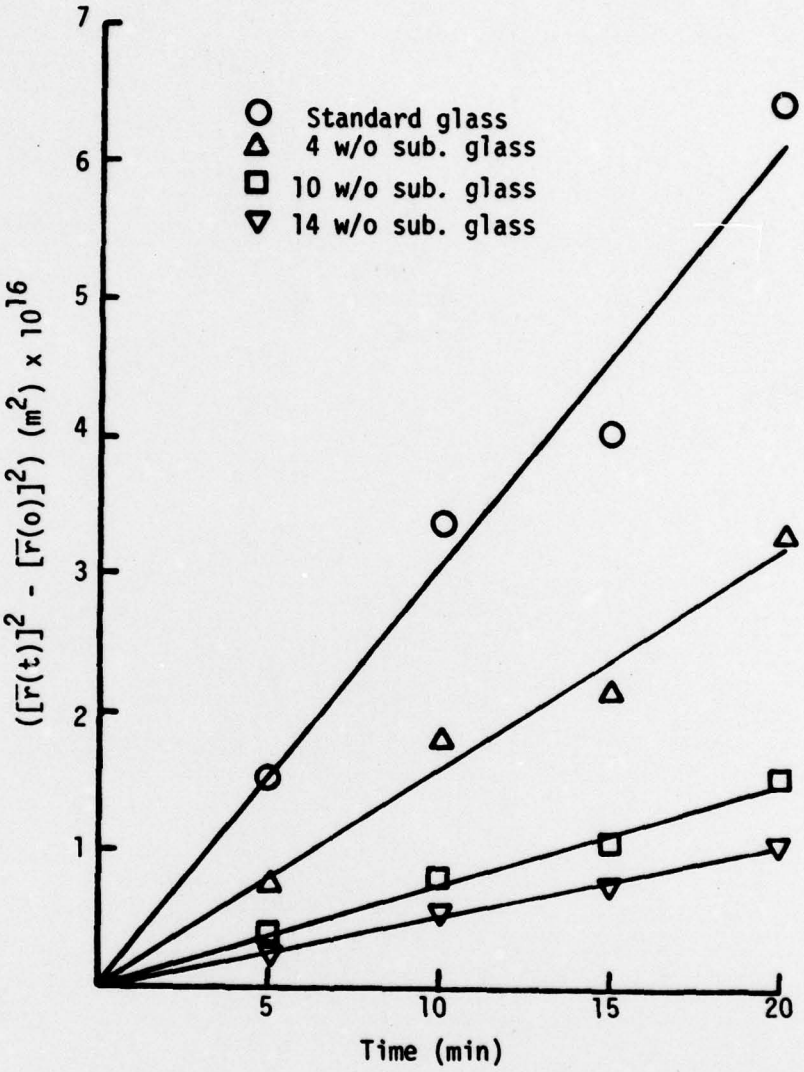

Rigure 5. RuO_2 Ripening in Glasses at 1000°C.

one standard deviation. Using the average exponential, an average value of the pre-exponential for each glass was calculated. Utilizing these results, an empirical equation for $C_o\gamma_{sl}K_T$ as a function of weight percent dissolved substrate (P) and temperature was derived.

$$C_o\gamma_{sl}K_T = \left[\frac{17.29}{1 + .172\ P + .00686\ P^2}\right] \exp\ (-49626/T) \quad (13)$$

The $C_o\gamma_{sl}K_T$ values obtained from the slopes of the experimental lines (Figs. 3-5) and from Eq. 13 are compared in Fig. 6.

Knowing C_o from the RuO_2 solubility measurements [3] and taking γ_{sl} to be 20 $\mu J/cm^2$, K_T was calculated as a function of composition and temperature. The γ_{sl} value of 20 $\mu J/cm^2$ was suggested [7] to represent the solid-liquid interfacial energy of the MgO-CaO-SiO_2 system. The calculated values of K_T, listed in Table I, appear to go through a maximum near 4 w/o substrate doping for any given temperature. This anomalous behavior is probably due to the assumption that the interfacial energy is independent of glass composition. RuO_2 solubility results [3] showed that the activity of RuO_2 in glass increases rapidly with glass composition up to 2 w/o substrate doping; the interfacial energy may exhibit a composition dependence similar to that of the activity of RuO_2. Although the transfer coefficient could not be determined precisely from the ripening results, the product $C_o\gamma_{sl}K_T$ is sufficient to predict RuO_2 sintering based on a liquid-phase sintering model presented in the following section.

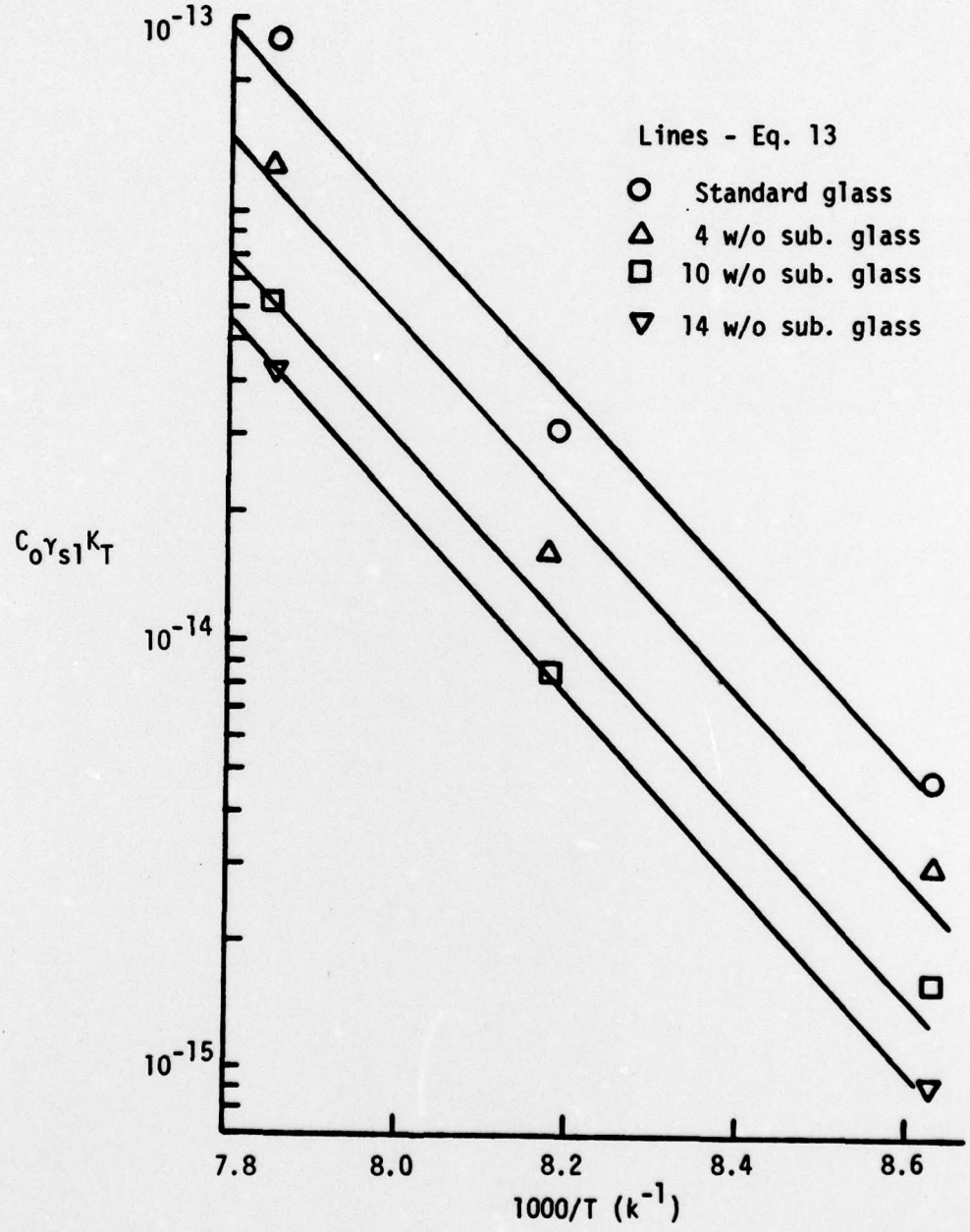

Figure 6. Variation of $C_o\gamma_{sl}K_T$ with Composition and Temperature.

TABLE I

Variation of K_T with Composition and Temperature

Composition	K_T (m/sec) x 10^7 at		
	888°C	950°C	1000°C
Standard Glass	5.61	28.3	191.0
4 w/o Sub. Glass	6.55	31.2	229.0
10 w/o Sub. Glass	3.45	16.0	107.0
14 w/o Sub. Glass	2.13	--	76.0

4. RuO_2 SINTERING

Consider a pair of spherical particles in contact, completely immersed in a liquid. If r is the radii of the particles, the concentration of species at the solid-liquid interface away from the neck region (C_1) relative to that at a flat interface (C_o) can be written as:

$$\ln = \frac{C_1}{C_o} = \frac{2\gamma_{sl} M}{r\rho RT}$$

If C_1 not much different from C_o, this equation can be approximated as:

$$C_1 - C_o \simeq \frac{2\gamma_{sl} M C_o}{r\rho RT} \qquad (14)$$

If x and y are the principal radii of curvature of the neck as shown in Fig. 7, the concentration of species in the neck region (C_2) relative to

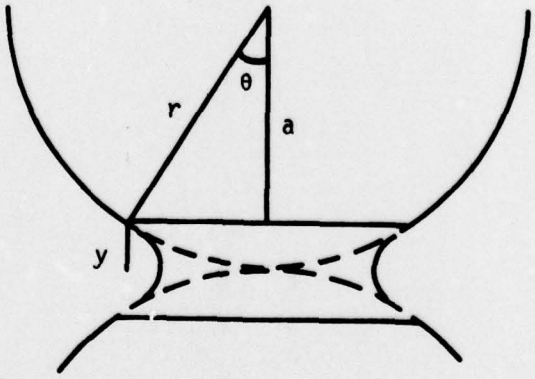

Figure 7. Geometry of Neck Between Particles Undergoing Liquid-Phase Sintering.

that at a flat interface is given by

$$\ln \frac{C_2}{C_o} = \frac{\gamma_{sl} M}{\rho RT}\left[\frac{1}{x} - \frac{1}{y}\right]$$

$$\simeq -\frac{\gamma_{sl} M}{\rho RT} \qquad \text{for } x >> y$$

$$C_2 - C_o \simeq -\frac{\gamma_{sl} M C_o}{y\rho RT} \tag{15}$$

In these equations, M is the molecular weight of the solid and ρ is the density of the solid. Combining Eqs. 14 and 15 gives

$$\Delta C = C_1 - C_2 \simeq \frac{\gamma_{sl} M C_o}{\rho RT}\left[\frac{2}{r} - \frac{1}{y}\right]$$

$$\Delta C \simeq \frac{\gamma_{sl} M C_o}{y\rho RT} \qquad \text{for } r >> y \tag{16}$$

If the neck growth between the particles is limited by the interface reaction, the rate of mass transfer, J(gm/s), can be written as

$$J = K_T A \Delta C \tag{17}$$

in which K_T (cm/s) is the transfer coefficient, A(cm^2) is the interfacial area, and ΔC(gm/cm^3) is the concentration difference between the free-surface and the neck area. For transport limited by redeposition at the neck, the interfacial area, A, in Eq. 17 is the neck area and from Fig. 7,

$$A \simeq 1/2(2\pi y)(2\pi x)$$

$$= 2\pi^2 xy$$

Substituting for A and ΔC in Eq. 17 gives

$$J = \frac{2\pi^2 x\ K_T\ \gamma_{sl}\ M\ C_o}{\rho RT} \tag{18}$$

By conservation of mass,

$$J = d\ (V_n \rho)/dt$$

where V_n is the neck volume. From Fig. 7,

$$V_n \simeq 1/2\ \pi x^2\ (2y)$$

and

$$y = (r - a) \simeq r(1 - \cos\theta) \simeq 2r\ \frac{\theta^2}{4} \simeq \frac{x^2}{2r}$$

Therefore,

$$J \simeq d\ (\frac{\pi x^4}{2r})\ \rho/dt$$

$$= \frac{2\pi\rho x^3}{r}\ dx/dt \tag{19}$$

Combining Eqs. 18 and 19 gives

$$x^2 dx = \frac{\pi K_T \gamma_{sl} M C_o\ r\ dt}{\rho^2 RT}$$

which integrates to

$$(\frac{x}{r})^3 = \frac{3\pi K_T \gamma_{sl} M C_o r^{-2} t}{\rho^2 RT} \tag{20}$$

If the neck growth is controlled by the diffusion of species through the liquid, the rate of mass transfer is given by

$$J = \frac{D\ A\ \Delta C}{0.78\ r} \tag{21}$$

in which $D(cm^2/s)$ is the diffusion coefficient of the slowest moving species

in the liquid, and 0.78 r is the average diffusion length which is taken to be equal to 1/8 of the periphery of the projected particle. Substituting for A and ΔC in Eq. 21, and by proceeding as for the interface controlled situation, it can be shown that

$$\left(\frac{x}{r}\right)^3 = \frac{3\pi D\gamma_{sl} MC_o r^{-3} t}{0.78\ \rho^2 RT} \simeq \frac{4\pi D\gamma_{sl} MC_o r^{-3} t}{\rho^2 RT} \qquad (22)$$

The effects of composition and temperature on the ripening of RuO_2 in glass was given by Eq. 13. By assuming that the transfer coefficient is the same for the ripening and the neck growth processes, the kinetics of neck growth between RuO_2 particles can be computed by combining Eqs. 20 and 13. The resulting equation is

$$x^3 = \frac{3\ Mrt}{\rho^2 RT} \frac{17.29 \times 10^5 \exp(-49626/T)}{(1 + 0.172P + 0.00686P^2)} \qquad (23)$$

The time required for the initial stage sintering ($x/r = 0.3$) of RuO_2 particles of different sizes in the standard glass is given as a function of temperature in Table II. At 800°C, for particles of 5 nm (50 Å) radius, it takes about 165 seconds to complete the initial stage sintering; whereas for particles of 1 μm radius, it takes nearly 2 1/2 months to achieve the same ratio of neck to particle radius. The effect of temperature on the neck growth process, as indicated by the high activation energy for ripening, is tremendous. For example, the time required by 5 nm particles to complete the initial stage sintering is increased by a factor of 100 if the temperature is lowered from 800 to 700°C.

TABLE II

Calculated Initial Stage Neck Growth Kinetics of RuO_2 in the Standard Glass

Temperature °C	Time(s) for x/r = 0.3				
	r = 5 nm	r = 10 nm	r = 100 nm	r = 1 μm	r = 10 μm
650	2.60×10^5	1.04×10^6	1.04×10^8	1.04×10^{10}	1.04×10^{12}
700	1.73×10^4	6.92×10^4	--	--	--
750	1.50×10^3	6.01×10^3	--	--	--
800	1.65×10^2	6.58×10^2	--	--	--
850	1.65×10^2	6.58×10^2	--	--	--
900	3.49	1.39×10	1.39×10^3	1.39×10^5	1.39×10^7

The effect of glass composition on the neck growth kinetics is indicated by Eq. 23. Additions of 4, 10, and 14 w/o substrate to the standard glass increase the time required for the completion of initial stage sintering by factors of approximately 2, 3.5, and 5, respectively. Equation 23 also indicates that for a given glass composition, temperature, and time, the neck size would be proportional to the 1/3 power of the particle size. The neck size calculated as a function of RuO_2 particle size and sintering temperature for a 10 minute sintering in the standard glass is given in Table III. A comparison of Tables II and III indicates that although larger particles take longer times (proportional to the square of their size) to complete the initial stage sintering ($x/r = 0.3$), they can achieve, for a given time, a larger neck radius (proportional to $r^{1/3}$) than the smaller particles.

TABLE III

Dependence of Neck Size on Particle Size and Temperature

Temperature °C	Neck Size (x) in nm for t = 10 min.				
	r = 5 nm	r = 10 nm	r = 100 nm	r = 1 μm	r = 10 μm
650	0.199	0.250	0.539	1.161	2.502
700	0.490	0.617	1.330	2.865	6.174
750	1.106	1.394	3.002	6.468	13.94
800	>1.5*	2.914	6.277	13.52	29.14
850	>1.5*	>3.0*	12.28	26.46	57.02
900	>1.5*	>3.0*	22.68	48.86	105.2

* Neck growth calculations using Eq. 23 are valid for $x/r \leq 0.3$ only.

5. FUTURE WORK

All experimental work on this contract has been completed. The results from studies of glass viscosity, surface tension and density, substrate dissolution rate, and RuO_2 solubility and ripening will be correlated utilizing the previously developed models for microstructure development, and the influence of glass composition established. The effects of substrate dissolution on charge transport processes in nonsintered contacts will be modeled, and the dependence of both the glass properties and the electrical properties of the nonsintered contacts on glass composition will be incorporated into a revised charge transport model for thick film resistors.

6. REFERENCES

1. R. W. Vest, "The Effects of Substrate Composition on Thick Film Circuit Reliability," Final Technical Report on Contract No. N0019-76-C-0354, 28 February 1977.

2. R. W. Vest, "The Effects of Substrate Composition on Thick Film Circuit Reliability," Final Technical Report on Contract No. N0019-77-C-0327, 28 February 1978.

3. R. W. Vest, "The Effects of Substrate Composition on Thick Film Circuit Reliability," Final Technical Report on Contract No. N0019-78-C-0236, 28 February 1979.

4. R. W. Vest, "The Effects of Substrate Composition on Thick Film Circuit Reliability," Quarterly Report No. 1 on Contract No. N0019-79-C-0240, 1 May 1979.

5. R. W. Vest, "The Effects of Substrate Composition on Thick Film Circuit Reliability," Quarterly Report No. 2 on Contract No. N0019-79-C-0240, 31 August 1979.

6. G. W. Morey, "Properties of Glass," Amer. Chem. Soc. Monograph No. 77, Reinhold, New York (1938).

7. J. White in "Science of Ceramics," Vol. II, G. H. Stewart, ed., Academy Press, London (1964).

7. STATEMENT OF ESTIMATED COSTS

Contract No. N0019-79-C-0240

February 1, 1979 - January 31, 1980

Beginning Fund Balance	$ 40,000.00
Funds Expended Through 10/31/79	32,079.00
Funds Remaining	$ 7,921.00

Planned Expenditures (Approximate)

November	$3,420
December	$2,275
January	$2,225